

www.batteries-supercaps.org



Check for updates

Special A Novel High-Performance Electrolyte for Extreme Fast Charging in Pilot Scale Lithium-Ion Pouch Cells

Zhijia Du,*[a] Zhenzhen Yang,[b] Runming Tao,[a] Vadim Shipitsyn,[c, d] Xianyang Wu,[a, b] David C. Robertson, [b] Kelsey M. Livingston, [a] Shae Hagler, [a] James Kwon, [a] Lin Ma, [c, d] Ira D. Bloom, [b] and Brian J. Ingram[b]

Realizing extreme fast charging (XFC) in lithium-ion batteries for electric vehicles is still challenging due to the insufficient lithium-ion transport kinetics, especially in the electrolyte. Herein, a novel high-performance electrolyte (HPE) consisting of lithium bis(fluorosulfonyl)imide (LiFSI), lithium hexafluorophosphate (LiPF₆) and carbonates is proposed and tested in pilotscale, 2-Ah pouch cells. Moreover, the origin of improved electrochemical performance is comprehensively studied via various characterizations, suggesting that the proposed HPE exhibits high ionic conductivity and excellent electrochemical stability at high charging rate of 6-C. Therefore, the HPE-based pouch cells deliver improved discharge specific capacity and excellent long-term cyclability up to 1500 cycles under XFC conditions, which is superior to the conventional state-of-theart baseline electrolyte.

Introduction

Lithium-ion batteries (LIBs) play an indispensable role in our modern life as the power portable electronics and electrical vehicles (EV). $\sp(1)$ Their overall performance improvements, such as higher energy/power density, lowers cost, and longer cycle life, seem to never cease. Although the cost of LIBs has dropped significantly in the past decade, the EV market is still a small portion of the light-duty vehicle sales compared to traditional internal combustion engine vehicles. In a report to the U.S. Department of Energy (DOE), the ability for EVs to fast charge can fuel wider EV adoption.[2] It is believed that having fast charging capability in EV batteries can help alleviate the "range anxiety," which is the main reason for consumers' hesitation to buy an EV. DOE has a goal of reducing charge time to 15 min or less and has defined extreme fast charging (XFC) as recharging up to 80% of the battery capacity in 10 min or less.[2]

Fast charging has introduced new challenges that need to be addressed in current EV batteries. In battery technology, a power cell, which has high power density, can be readily used

- [a] Dr. Z. Du, Dr. R. Tao, Dr. X. Wu, K. M. Livingston, S. Hagler, J. Kwon Electrification and Energy Infrastructure Division, Oak Ridge National Laboratory, 37830 Oak Ridge, TN, USA E-mail: duz1@ornl.gov
- [b] Dr. Z. Yang, Dr. X. Wu, D. C. Robertson, Dr. I. D. Bloom, Dr. B. J. Ingram Chemical Sciences and Engineering Division, Argonne National Laboratory, 9700 S Cass Ave, 60439 Lemont, IL, USA
- [c] V. Shipitsvn, Prof. Dr. L. Ma Department of Mechanical Engineering and Engineering Science, The University of North Carolina at Charlotte, 28223 Charlotte, NC, USA
- [d] V. Shipitsyn, Prof. Dr. L. Ma Battery Complexity, Autonomous Vehicle and Electrification (BATT CAVE) Research Center, The University of North Carolina at Charlotte, 28223 Charlotte, NC, USA
- Supporting information for this article is available on the WWW under https://doi.org/10.1002/batt.202300292

An invited contribution to a Special Collection on Fast Charging Batteries

in a fast-charging scenario. However, a power cell utilizes thin electrodes that can lead to low energy density and high cell cost. Thicker electrodes in an energy cell with higher areal capacity can increase the energy density and reduce cost.[3-5] The cost for 85-kWh pack has been estimated to be \$107/kWh for cells with 87-μm anode compared to \$196/kWh with 1-μm anode. Thus, it is thus ideal for an EV to have energy cells from a cost and driving range perspective. However, the main drawback of energy cells is the inability to charge quickly. Mass transfer of lithium ions (Li⁺) takes place from cathode to anode through the porous electrodes, electrolyte and separators during charging. With the increase of charging rate, this mass transfer needs to be completed faster, or in shorter time. In thick electrodes, the limitation of Li⁺ mass transfer from low conductivity and low Li⁺ transference numbers leads to the depletion of Li⁺ in electrolyte. [6-9] Li⁺ depletion can lead to metallic Li plating, and even dendritic Li growth on graphite anode, which causes the consumption active Li⁺ and eventually leads to capacity decay and/or safety issues under fast charging conditions.[2,4,10,11]

To resolve the XFC issues, scientists have proposed several approaches. Yang et al. proposed that increase the charging temperature can increase the movement of Li⁺ and, thus, improves the fast charging cell performance. [12,13] However, it might be challenging to integrate an extra heating system to the EV battery pack due to the limited space and additional consumption of energy. An obvious route to address the XFC challenges is the electrolyte formulation, which can improve the mass transfer kinetics of Li+ and facilitate the Li+ intercalation into graphite. Notably, a few years ago, our group first reported that a lithium bis(fluorosulfonyl)imide (LiFSI)based electrolyte can dramatically enhance the ionic conductivity and Li⁺ transference number due to the higher dissociation of the LiFSI salt in the electrolyte and the larger size of the FSIanion.[10,14,15] Additionally, the multiphysics simulation from Colclasure et al. suggests that the identified key factors of the transport properties of electrolyte for fast charging without Li plating are ionic conductivity, diffusivity and transference number. Therefore, inspired from the pioneering work, developing a new high-performance electrolyte system and validating the performance in pilot-scale pouch cells for XFC is essential.

Herein, a novel high-performance electrolyte (HPE) for the XFC application is proposed. The proposed electrolyte is a matrix of LiFSI, LiPF₆ and carbonates. Electrolytes using the LiFSI salt have been shown to improve the ionic conductivity due to a higher degree of dissociation than LiPF₆. To, 189 The addition of LiPF₆ in the LiFI-based electrolyte formulation has shown to be beneficial to battery performance. The HPE electrolyte contains 30 wt% dimethyl carbonate (DMC). DMC has a lower viscosity (0.59 cP) and higher dielectric constant (3.12) compared to ethyl methyl carbonate (EMC) (viscosity of 0.65 cP and dielectric constant of 2.9). Electrolytes with a lower viscosity will have a higher conductivity because the ions move more easily. A higher dielectric constant will also improve conductivity as it shields the ions from the attraction of ions with opposite charge, thus preventing ion pairing in the electrolyte.

The performance of HPE electrolyte is then demonstrated in a 2-Ah, pilot-scale pouch cell, which is an important step for the realization of new battery technology from laboratory scale to industry. [21-23] Indeed, the developed HPE delivers better performance than the state-of-the-art Gen2 electrolyte. Moreover, the chemistry of the formed cathode electrolyte interphase (CEI) layers and solid electrolyte interphase (SEI) layers is probed for the very first time, demonstrating the proposed HPE can lead to robust electrolyte passivation layer for long-term cycling under XFC conditions. Therefore, this work not only suggests that the developed HPE electrolyte should be considered as a promising candidate for EV XFC applications due to the observed superb electrochemical performance and material accessibility, but also would potentially enlighten the research and development of electrolyte for high-performance LIBs.

Results and Discussion

Figure 1 shows the ionic conductivities of electrolytes in this study. In the baseline Gen2 electrolyte, LiPF₆ is the salt of choice due to its balance of low cost, high ionic conductivity, relative stability, and relatively high degree of dissociation in carbonate solvents.[24] However, fast charging of LIBs has demanded electrolyte formulations with higher ionic conductivity and higher Li⁺ transference numbers. LiFSI has been shown to improve the ionic conductivity due to a higher degree of dissociation than LiPF₆. ^[10,18] The HPE electrolyte also has 30 wt% of DMC to lower its viscosity and increase its higher dielectric constant over those of EMC. [20] With all these factors combined, HPE electrolyte shows consistent improvement of ionic conductivity compared to Gen2 electrolyte. Both electrolytes show increase of conductivity at elevated temperature, which can be attributed to the added thermal agitation that weakens the ion pairing and decreases viscosity. Previous reports have found

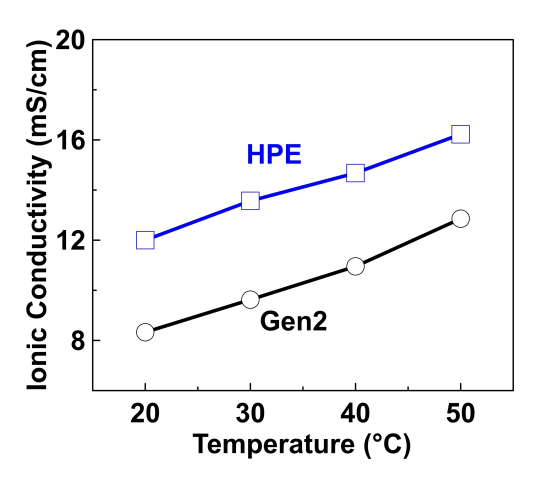


Figure 1. Ionic conductivities of HPE electrolyte and Gen2 electrolyte at different temperatures.

that cell temperature can increase considerably from the heat generation during fast charging.^[13,25] Therefore, the improvement in electrolyte conductivity at higher temperature will be beneficial towards fast charging application. Li ion transference number (tLi⁺) measurement confirmed that HPE electrolyte has a tLi⁺ of 0.5, which is much higher than tLi⁺ of 0.3 for Gen2 electrolyte.

Figure 2(a) shows the self-heating rate (SHR) versus temperature results for 2.5-mAh of lithiated graphite heated with 7 mg electrolyte between 50 °C and 350 °C. Compared to the Gen2 control electrolyte, HPE electrolyte shows a similar reactivity across a wide temperature range, which indicates that the use of HPE electrolyte will not compromise the thermal stability of anode material. Figure 2(b) shows the SHR versus temperature results for 2.5 mAh of delithiated NMC heated with 7 mg electrolyte between 50 °C and 350 °C. It is worth noting that the use of HPE electrolyte increases the onset temperature from ~100 °C to ~140 °C compared to the Gen2 electrolyte. Generally, the use of HPE electrolyte will improve the thermal stability

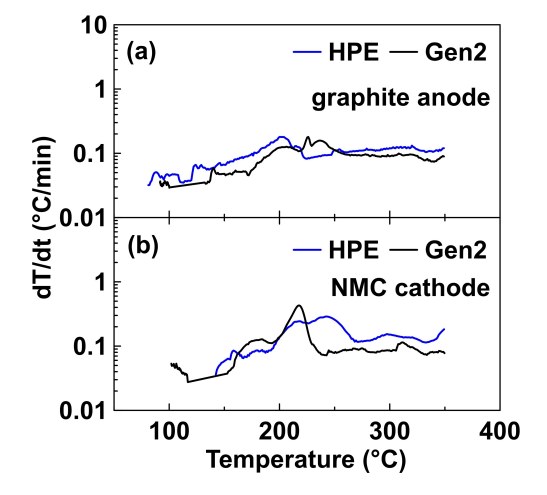


Figure 2. Self-heating rate vs. temperature for a) lithiated graphite and b) de-lithiated NMC reacting with HPE electrolyte compared with the Gen2 control electrolyte. These experiments used 2.5 mAh (NMC) and 2.5 mAh (graphite) electrode and ~7 mg electrolyte.

under the lean electrolyte condition from the perspective of cathode.

Figure 3(a) shows the voltage and current curves for 2-Ah pouch cells filled with the HPE and Gen2 electrolyte. Under the 6 C charging rate, the cell voltages gradually increase during the constant current (CC) charging and reached the cutoff voltage (4.2 V) in around 2.6 min (Gen2) and 5.6 min (HPE). The cells are further charged using the constant voltage mode with a decreasing trickle current until the overall charging time reaches 10 min. The large gap (shaded areas in Figure 3a) between the plots of current vs. time indicates that more capacity can be stored when the cell has a longer CC charging time. A calculation (similar to our prior report^[10]) shows that a 60-Ah LIB filled with the HPE electrolyte would achieve energy density of 180 Wh/kg, which is much higher than 156 Wh/kg obtained with Gen2 electrolyte.

Figure 3(b) shows the cycling performance of the 2-Ah pouch cells under different C rates. HPE electrolyte shows excellent cycling performance under standard C/3 charge/ discharge with 92.2% of capacity retention after 700 cycles. This demonstrates HPE electrolyte has no adverse effect on standard C/3 rate battery operations. Under 10-minute XFC protocol, 2-Ah pouch cell with HPE electrolyte delivers 1.54 Ah capacity, which is ~15% higher than 1.34 Ah from the cell with Gen2 electrolyte. This can be ascribed to the improved Li⁺ mass transfer properties as discussed earlier. The cells with both

electrolytes show similar cycling performance with HPE cell capacity retention of 92.3 % and 90.6 % from the Gen2 cell after 500 XFC cycles. A calculation of the cell energy density yields 166 Wh/kg for cells with HPE, which is much higher than DOE's target of 144 Wh/kg after 500 XFC cycles. With further cycling of the cells, HPE-based cell can still deliver 80.2 % of capacity after 1500 cycles, which triples the cycle life of capacity retention criteria in DOE's target (80 % after 500 cycles). It is also much higher than that of the Gen2-based cells, which has 72.1 % capacity retention after 1500 cycles.

Figure 4 shows the cell resistance before and after 1500 XFC cycles as measured using the Hybrid pulse power characterization test (HPPC). By comparing the discharge voltage profile, the cell with HPE electrolyte has ~9% capacity loss when charged at C/3 rate after XFC cycles, and the cell with Gen2 electrolyte has twice of capacity loss of ~18%. This demonstrates the superior capacity retention using HPE electrolyte when the cell is switched back at C/3 standard rate even after 1500 XFC cycles. Similar cell resistances are observed in both cells except the HPE cell is a consistently lower by a small value. The cell resistance with Gen2 increases significantly by ~69% at 80% SOC after repeated XFC cycles. The resistance increase with HPE electrolyte is much lower at ~34% at 80% SOC. HPE electrolyte has demonstrated as a better electrolyte for fast charging due to its ability to retain more capacity and gain smaller increase in cell resistance after repeated XFC cycles.

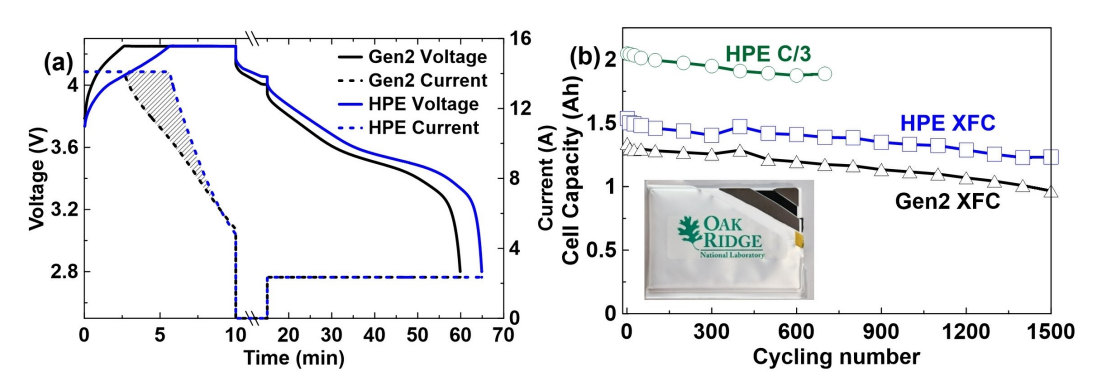


Figure 3. a) Voltage and current versus charging time for cells charged at the 6 C with a time cutoff of 10 min and discharged at the 1 C rate. b) Long-term cycling performance of 2-Ah pouch cells filled with different electrolytes cycled at C/3 standard rate and XFC protocols.

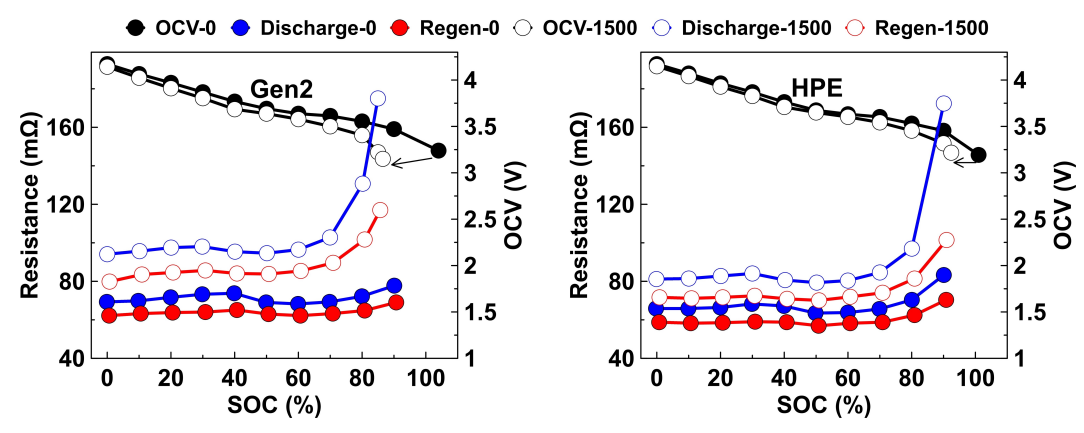


Figure 4. OCV and cell resistances from HPPC test before and after 1500 XFC cycles for cells filled with a) Gen2 and b) HPE electrolyte.

and-conditions) on Wiley Online Library for rules of use; OA articles are governed by the applicable Creative Commons

25666223, 20

3, 10, Downloaded from https://chemistry-europe.onlinelibinary.wiley.com/doi/10.1002/butt.202300202 by University of North Carolina, Wiley Online Library on [03/06/2024]. See the Terms and Conditions (https://onlinelibinary.wiley.com/terms-and-conditions) on Wiley Online Library for rules of use; OA archies are governed by the applicable Creative Commons Licenses

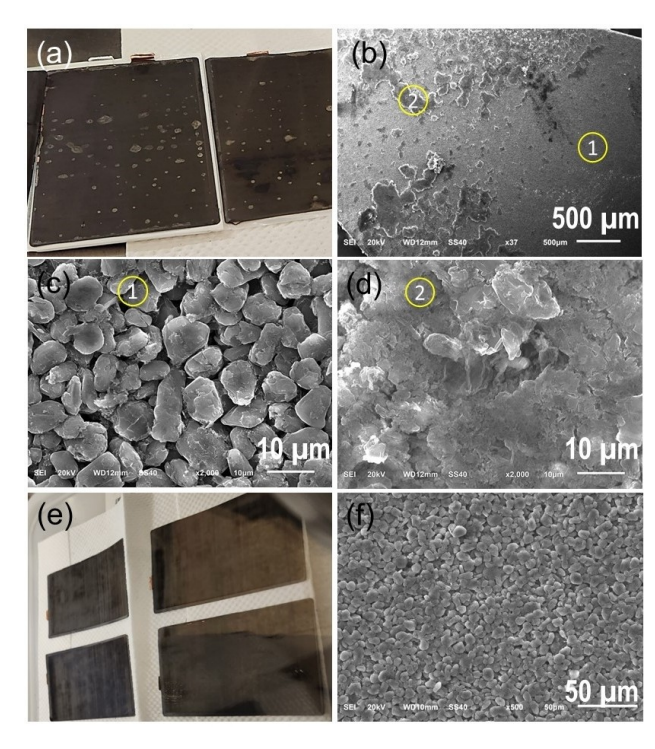


Figure 5. a) Optical and b-d) SEM images of graphite electrode from Gen2 cell after 1500 XFC cycles (1) is area without Li plating, and 2) is area with Li plating). e) Optical and f) SEM images of graphite electrode from HPE cell.

Figure 5 shows the optical and SEM images of graphite electrodes in 2-Ah pouch cell with different electrolytes after 1500 XFC cycles. For Gen2 electrolyte, small areas of Li plating can be clearly seen across the electrode surface. The graphite electrode with Li plating and without Li plating can be easily distinguished by SEM as area 2 and 1, respectively. The severity of Li plating is less than a previous report by Gallagher et al. even though the same electrode loading and electrolyte are used. [4] A big difference is the size of the cells: 2-Ah pouch cell with multilayer double sides electrodes in this study, versus ~50 mAh pouch cell with single layer single sided electrode in Ref. [4]. Errors can be magnified or accumulated in small cells that lead to severe Li plating, which proves the importance of having a high capacity LIB cell (2-Ah cell in this case) for performance verification and validation. No Li plating is spotted for electrodes with HPE electrolyte, which is mainly ascribed to its improved Li⁺ mass transfer properties. The SEM images of the NMC cathode are shown in Figure S1. There is no clear difference in morphologies of the electrode from Gen2 cell and HPE cell.

To understand what effect the HPE had on the surface chemistry of the electrode, the SEI layer on graphite anode (Figure 6) and CEI layer on NMC622 cathode (Figure 7) are analyzed by XPS. Typically, an electrolyte goes through various chemical/electrochemical reactions, including oxidation and reduction at the positive and negative electrodes,

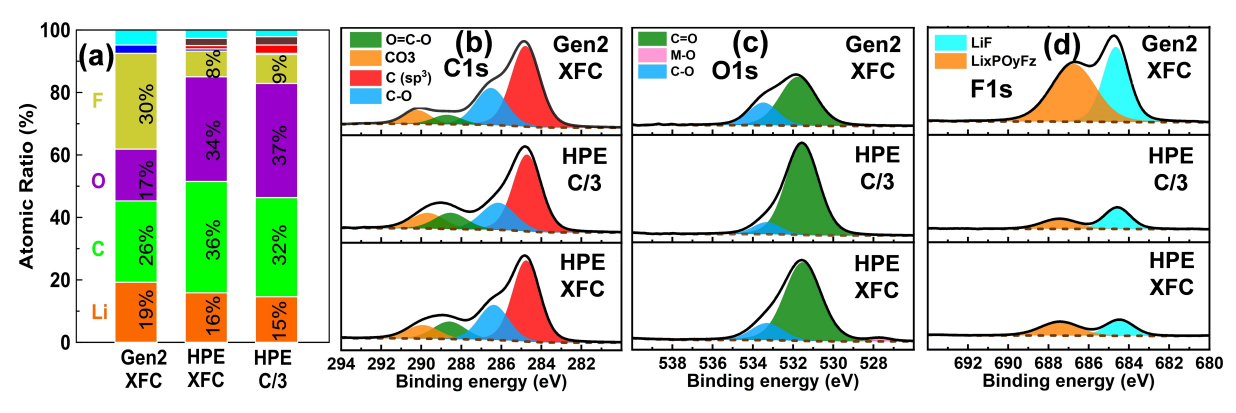


Figure 6. XPS analyses for SEI layers. a) XPS survey atomic ratio. B-d) C-1 s, O-1 s and F-1 s HRXPS spectra (700 cycles at C/3 for ORNL electrolyte, and 1500 cycles at XFC for both Gen2 and HPE electrolytes).

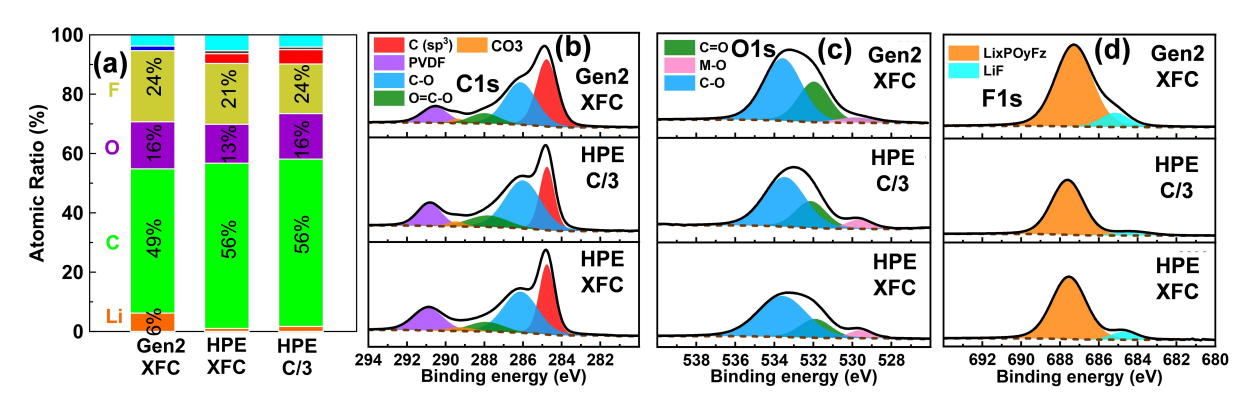


Figure 7. XPS analysis for CEI layers. a) XPS survey atomic ratio. b-d) C-1 s, O-1 s and F-1 s HRXPS spectra (700 cycles at C/3 for ORNL electrolyte, and 1500 cycles at XFC for both Gen2 and HPE electrolytes).

Chemistry Europe European Chemical Societies Publishing

respectively,[24] leading to the formation of inorganic species (Li₂CO₃, LiF, Li₂O, Li_xPO_vF_z and Li_xPF_v) and organic compounds (such as (CH2OCO2Li)2, other organic carbonates (R2CO3), polyethylene glycol (PEO) oligomer, etc.).[26-31] Figure 6(a) shows the concentration of each element in the SEI layers. It exhibits the C-rich and O-rich feature for ORNL electrolyte, and Li-rich and F-rich feature for Gen2 electrolyte. Additionally, the composition of the two SEI layers formed from HPE at different current densities is highly similar, implying that HPE electrolyte exhibits excellent electrochemical stability at high rate. Figures 6(b-d) shows similar C 1s, O 1s and F 1s high-resolution XPS (HRXPS) results for all three electrodes (Figure S2 shows the P 2p, N 1s and S 2p HRXPS results). One noticeable difference is the F 1s, where HPE cell shows much lower intensity than Gen2 cell. The results suggest that HPE has less salt decomposition than Gen2 does during cycling, which is in line with the lower F content of the SEI in HPE cell in Figure 6(a). The difference of the SEI composition probably would affect the Li ion diffusion through the SEI layer. A recent study suggests that the Li ion diffusivity in amorphous Li₂CO₃ is at least 1 order of magnitude higher than that in LiF.[32] They also found LiF-rich SEI can inhibit efficient Li ion diffusion, leading to high overpotentials and poor rate performance. In our study, the SEI from HPE cell shows more carbonates and less LiF than Gen2 cell. This may improve the Li ion diffusion in the SEI layer in HPE cell, and thus enhance the XFC capability.

Figure 7(a) shows the elemental compositions of CEI after cycling. Electrode with Gen2 electrolyte shows higher Li content, further confirming extensive Li salt decomposition in Gen2. This agrees with F 1s HRXPS in Figure 7(d) where Li_xPO_yF_z and LiF (from salt decomposition) has higher intensity for Gen2 compared to HPE. In the O 1s HRXPS results in Figure 7(c), the peak at ~529.5 eV can be attributed to M-O from the lattice oxygen in NMC622,[33] the peak at ~531.7 is ascribed to C=Olike oxygen from carbonate compounds (such as ROCO₂Li), [34] and the peak at \sim 533.5 eV is assigned to -C-O- bonds from ether derivatives.[35-37] The M-O peak almost disappears due to the thick CEI layer formed from Gen2, indicating that the degradation of Gen2 is more severe than that of HPE, thereby which illustrates the excellent electrochemical stability of HPE.

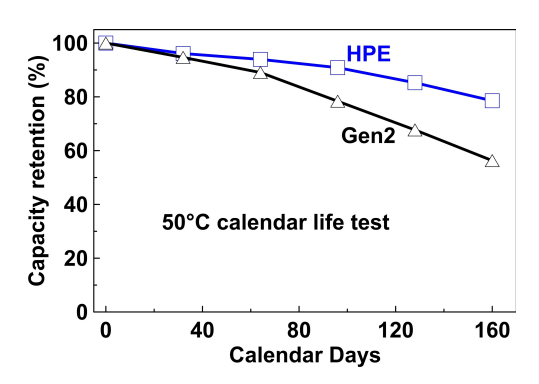


Figure 8. High temperature (50 °C) calendar life testing of 2-Ah pouch cells with Gen2 and HPE electrolyte.

The thick electrolyte passivation layer in Gen2 cell can impede the Li⁺ transport kinetics, resulting in poor rate capability. Thereby, such observation is consistent with the obtained XFC tests above, implying the effectiveness of HPE for XFC LIB application.

Another important cell testing for fast charging is high temperature calendar life assessment. We have found that the temperature in a 2-Ah pouch cell can increase considerably during fast charging. [25] Figure 8 shows the calendar life of 2-Ah pouch cells with Gen2 and HPE electrolytes. After 160 days of high temperature (50 °C) life testing, the cell with HPE electrolyte still has 79% of original capacity, which is much higher than the 56% capacity retention for the cell with Gen2 electrolyte. LiPF₆ is known for its instability at high temperature, which produces HF with trace amounts water in electrolyte that can damage SEI and cell performance. [24,38] On the contrary, LiFSI has been demonstrated to be more stable at elevated temperatures. [39,40] The calendar life test at 50 °C proves that HPE electrolyte is better than Gen2 electrolyte when high temperature events occur during battery operation.

Figure 9 shows the cell resistance before and after 160 days calendar life test at 50 °C. By comparing the discharge voltage curve, the cell with HPE electrolyte has ~19% capacity loss while the cell with Gen2 cell has lost ~32% of its original capacity. This demonstrates the superior capability of using HPE

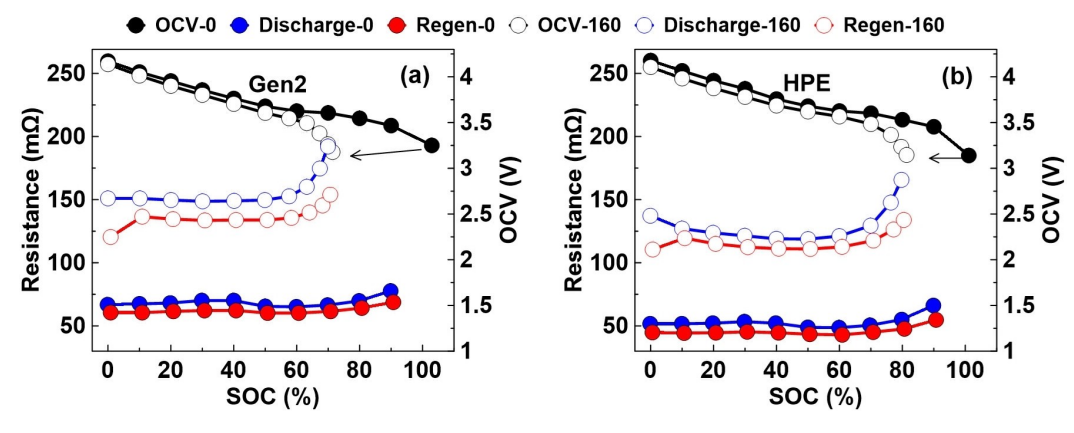


Figure 9. OCV and cell resistances from HPPC test before and after 160 days of high temperature (50°C) calendar life testing for cells filled with a) Gen2 and b) HPE electrolyte.



5666223,

electrolyte when the cell is exposed to high temperature operation. The increase of cell resistance for HPE cell after high temperature test is also much smaller than Gen2 cell. The cell resistance with Gen2 increases significantly by an average of $\sim 150\%$ after 160 days. The resistance increase with HPE electrolyte is much lower, $\sim 90\%$.

Conclusions

In conclusion, a novel high-performance LiFSI-LiPF₆-carbonate electrolyte system was successfully developed for XFC of LIBs. The proposed HPE, indeed, delivered excellent electrochemical performance in the 2-Ah, pilot-scale pouch cells, which is highly practical and transferable for EV applications. Such achievement is rooted in the desirable electrochemical and thermal stability of HPE and the high Li⁺ conductivity. Therefore, it is believed that this work not only establishes a new HPE for fast-rechargeable LIBs, but also establishes some fundamental understanding that can potentially enlighten the research and development of next-generation electrolytes.

Experimental Section

Electrolyte formulation: Electrolyte and solvents used in the study were purchased from SoulBrain MI. The baseline Gen2 electrolyte is 1.2 M LiPF₆ in ethylene carbonate (EC)/ EMC 30/70 wt%. The HPE for fast charging was formulated by first dissolving 1.5 M LiFSI into a solvent mixture of EC, EMC and DMC at a ratio of 40/30/30 wt%. Then, 10 wt% of Gen2 electrolyte was added to obtain the final product. Karl-Fisher titration (Mettler Toledo) was carried out to verify the water content (<25 ppm) in the electrolyte. Ionic conductivity was measured using a conductivity cell (Cole-Parmer), which was calibrated using standard KCl solutions. The conductivities were measured using electrochemical impedance spectroscopy (EIS) from 10 Hz to 1 MHz with a 6 mV perturbation voltage using a potentiostat (Bio-Logic).[10] Li ion transference number was measured using Li/Li symmetric cell filled with HPE electrolyte or Gen2 electrolyte. A voltage bias of 5 mV was applied during the potentiostatic polarization experiments, and the impedances were measured in the frequency range of 1-100 kHz with a 5 mV perturbation voltage using a Bio-Logic potentiostat. [10]

Preparation of pouch cells: The NMC622 and graphite electrodes are prepared in a dry room (with a dew point of less than 50 °C and a relative humidity of 0.1%) in the Battery Manufacturing Facility at Oak Ridge National Laboratory. The graphite anode consisted of 94 wt.% graphite (Superior Graphite 1520T), 1 wt.% carbon black (Timical C65) and 5 wt.% polyvinylidene fluoride (PVDF, Kureha 9300). The areal loading was 3.30 ($\pm\,0.05)\,\text{mAh/cm}^2$ with a porosity of 30% after calendering. The cathode consisted of 94 wt.% NMC622 (Targray), 3 wt.% carbon black (Denka Li-100) and 3 wt.% polyvinylidene fluoride (PVDF, Solvay 5130), with an areal loading of 2.90 (\pm 0.05) mAh/cm² and porosity of 30% after calendering. The multi-layered pouch cells were assembled with cathodes and anodes stacking together separated by separators (Celgard® 2325). The pouch cells were filled with electrolyte in the dry room and vacuum sealed. The electrolyte volume factor is 1.2, which is defined as the supplied electrolyte volume divided by the total cell pore volume (the sum of pore volumes in anode, cathode and separator). The cells were placed in between two aluminum plates

and bolted down with a pressure of 4 psi on the cells. The nominal capacity of the pouch cells was 2.00 $(\pm\,0.05)$ Ah.

Accelerating rate calorimetry (ARC) test: To prepare high state-ofcharge electrodes for thermal stability testing, NMC/graphite coin cells were prepared and charged to 4.2 V at the C/40 rate. Once reaching 4.2 V, the cells were allowed to relax under open-circuit conditions for 15 min. The cells were charged to 4.2 V again, using half of the original current, C/80. After four such cycles, where the current was reduced a factor of two each time, the charged cells were transferred to the glove box and dissembled to obtain the lithiated graphite electrodes and de-lithiated NMC electrodes. Samples (1 cm²) of delithiated NMC electrode (~2.5 mAh) or lithiated graphite electrode (~2.5 mAh) were sealed with ~7 mg electrolyte in a stainless-steel tube with tungsten inert gas welding inside an Ar-filled glovebox. This will mimic the lean electrolyte condition. The sample was then set on the thermocouple of an accelerating rate calorimeter for following characterization. The ARC starting and ending temperatures were set at 50 °C and 350 °C, respectively, to cover a wide temperature range. ARC tests were tracked under adiabatic conditions when the sample SHR exceeded 0.03 °C/min. ARC testing was set to be automatically stopped at either 380 °C or when the SHR exceeded 10 °C/min for 0.5 min.

Cell performance validation: The pouch cells first went through four formation charge/discharge cycles at the C/20 rate in the voltage range of 3.0 and 4.2 V. Following formation cycling, the cells were degassed and resealed under vacuum. The cells were cycled between 2.8 and 4.2 V with a constant voltage hold at 4.2 V (trickle charging). For XFC, a total time limit of 10 minutes was imposed during charge to guarantee that the duration of the charging step did not exceed the intended time, and discharge was conducted at the 1-C rate. Standard cycle life test was performed on cells with HPE electrolyte at C/3 charge/discharge rate. High temperature calendar life was tested at 50 °C. HPPC was performed at the 1-C rate (referred as low current HPPC test). Details on the testing procedure and terminologies can be found in Battery Test Manual For Electric Vehicles by J. P. Christopherson. [41]

Post-mortem analysis: The cycled pouch cells were opened in an Ar-filled glove box for post-mortem analysis. The SEM images of aged graphite anodes were obtained using a JEOL JSM-6610LV SEM at 20.0 kV. X-ray photoelectron spectroscopy (XPS) was conducted on the harvested electrodes using a PHI 5000 XPS VersaProbe II system manufactured by Physical Electronics. The system was connected to an Ar-atmosphere glovebox, and the samples were introduced into the XPS analysis chamber through the glovebox, ensuring no exposure to air. The core-level spectra were acquired using an Al K_{α} radiation beam (hv=1486.6 eV) with a beam diameter of 100 μ m, a power of 25 W, and an electron-beam sample neutralizer. All core-level spectra were referenced to the C1s hydrocarbon peak at 284.8 eV.

Acknowledgements

This research at Oak Ridge National Laboratory, managed by UT Battelle, LLC, for the U.S. Department of Energy (DOE) under contract DE-AC05-00OR22725, was sponsored by the Office of Energy Efficiency and Renewable Energy (EERE) Vehicle Technologies Office (VTO) (Program Manager: Brian Cunningham, Technology Manager: Jake Herb). Argonne National Laboratory is operated for the DOE Office of Science by UChicago Argonne, LLC, under contract number DE-AC02-06CH11357. L. M. ac-

Chemistry Europe European Chemical Societies Publishing

5666223,

knowledges the support by the US National Science Foundation Award No. 2301719.

Note: This manuscript has been authored by UT-Battelle, LLC under Contract No. DE-AC05-00OR22725 with the U.S. Department of Energy. The United States Government retains and the publisher, by accepting the article for publication, acknowledges that the United States Government retains a non-exclusive, paid-up, irrevocable, world-wide license to publish or reproduce the published form of this manuscript, or allow others to do so, for United States Government purposes. The Department of Energy will provide public access to these results of federally sponsored research in accordance with the DOE Public Access Plan (http://energy.gov/downloads/doepublic-access-plan).

Conflict of Interests

The authors declare no conflict of interest.

Data Availability Statement

The data that support the findings of this study are available from the corresponding author upon reasonable request.

Keywords: calendar life \cdot electrolyte \cdot fast charging \cdot post-test \cdot pouch cell

- [1] J. B. Goodenough, Nat. Electron. 2018, 1, 204.
- [2] D. Howell, S. Boyd, B. Cunningham, S. Gillard, L. Slezak, S. Ahmed, I. Bloom, A. Burnham, K. Hardy, A. N. Jansen, P. A. Nelson, D. C. Robertson, T. Stephens, R. Vijayagopal, R.B. Carlson, F. Dias, E.J. Dufek, C.J. Michelbacher, M. Mohanpurkar, D. Scoffield, M. Shirk, T. Tanim, M. Keyser, C. Kreuzer, O. Li, A. Markel, A. Meintz, A. Pesaran, S. Santhanagopalan, K. Smith, E. Wood, J. Zhang, 2017. DOE report. https://energy.gov/sites/prod/files/2017/10/f38/XFC Technology Gap Assessment Report_FINAL_10202017.pdf.
- [3] D. L. Wood, J. Li, C. Daniel, J. Power Sources 2015, 275, 234.
- [4] K. G. Gallagher, S. E. Trask, C. Bauer, T. Woehrle, S. F. Lux, M. Tschech, P. Lamp, B. J. Polzin, S. Ha, B. Long, Q. Wu, W. Lu, D. W. Dees, A. N. Jansen, J. Electrochem. Soc. 2016, 163, A138.
- [5] S. Ahmed, I. Bloom, A. N. Jansen, T. Tanim, E. J. Dufek, A. Pesaran, A. Burnham, R. B. Carlson, F. Dias, K. Hardy, M. Keyser, C. Kreuzer, A. Markel, A. Meintz, C. Michelbacher, M. Mohanpurkar, P. A. Nelson, D. C. Robertson, D. Scoffield, M. Shirk, T. Stephens, R. Vijayagopal, J. Zhang, J. Power Sources 2017, 367, 250.
- [6] H. J. Chang, A. J. Ilott, N. M. Trease, M. Mohammadi, A. Jerschow, C. P. Grey, J. Am. Chem. Soc. 2015, 137, 15209.
- [7] J. H. Cheng, A. A. Assegie, C. J. Huang, M. H. Lin, A. M. Tripathi, C. C. Wang, M. T. Tang, Y. F. Song, W. N. Su, B. J. Hwang, J. Phys. Chem. C 2017, 121, 7761.
- [8] F. Orsini, A. Du Pasquier, B. Beaudoin, J. Tarascon, M. Trentin, N. Langenhuizen, E. De Beer, P. Notten, J. Power Sources 1998, 76, 19.
- [9] J. N. Chazalviel, Phys. Rev. A 1990, 42, 7355.
- [10] Z. Du, D. L. Wood, I. Belharouak, *Electrochem. Commun.* 2019, 103, 109.

- [11] Z. Yang, H. Charalambous, Y. Lin, S. E. Trask, L. Yu, J. Wen, A. Jansen, Y. Tsai, K. M. Wiaderek, Y. Ren, I. Bloom, J. Power Sources 2022, 521,
- [12] X. G. Yang, C. Y. Wang, J. Power Sources 2018, 402, 489.
- [13] X.-G. Yang, G. Zhang, S. Ge, C.-Y. Wang, Proc. Nat. Acad. Sci. 2018, 115, 7266.
- [14] X. Wu, Z. Du, Electrochem. Commun. 2021, 129, 107088.
- [15] X. Wu, L. Ma, J. Liu, K. Zhao, D. L. Wood, Z. Du, J. Power Sources 2022, 545, 231863.
- [16] A. M. Colclasure, A. R. Dunlop, S. E. Trask, B. J. Polzin, A. N. Jansen, K. Smith, J. Electrochem. Soc. 2019, 166, A1412.
- [17] A. M. Colclasure, T. R. Tanim, A. N. Jansen, S. E. Trask, A. R. Dunlop, B. J. Polzin, I. Bloom, D. Robertson, L. R. Flores, M. Evans, E. J. Dufek, K. Smith, Electrochim, Acta 2020, 337, 135854.
- [18] H. B. Han, S. S. Zhou, D. J. Zhang, S. W. Feng, L. F. Li, K. Liu, W. F. Feng, J. Nie, H. Li, X. J. Huang, M. Armand, Z. Bin Zhou, J. Power Sources 2011,
- [19] D. Y. Wang, A. Xiao, L. Wells, J. R. Dahn, J. Electrochem. Soc. 2015, 162, A169.
- [20] T. B. Reddy, in Linden's Handbook of Batteries, Fourth Edition, 2002.
- [21] V. Müller, R. Bernhard, J. Wegener, J. Pfeiffer, S. Rössler, R. G. Scurtu, M. Memm, M. A. Danzer, M. Wohlfahrt-Mehrens, Energy Technol. 2020, 8, 2000217.
- [22] S. Chen, C. Niu, H. Lee, Q. Li, L. Yu, W. Xu, J.-G. Zhang, E. J. Dufek, M. S. Whittingham, S. Meng, J. Xiao, J. Liu, Joule 2019, 3, 1094
- [23] S. E. Trask, Y. Li, J. J. Kubal, M. Bettge, B. J. Polzin, Y. Zhu, A. N. Jansen, D. P. Abraham, J. Power Sources 2014, 259, 233-244.
- [24] K. Xu, Chem. Rev. 2014, 114, 11503.
- [25] S. Huang, X. Wu, G. M. Cavalheiro, X. Du, B. Liu, Z. Du, G. Zhang, J. Electrochem. Soc. 2019, 166, 3254.
- [26] S. J. An, J. Li, C. Daniel, D. Mohanty, S. Nagpure, D. L. Wood, Carbon 2016, 105, 52.
- [27] K. Edström, T. Gustafsson, J. O. Thomas, Electrochim. Acta 2004, 50, 397.
- [28] G. Zhuang, Y. Chen, P. N. Ross, Langmuir 1999, 15, 1470.
- [29] R. Dedryvère, H. Martinez, S. Leroy, D. Lemordant, F. Bonhomme, P. Biensan, D. Gonbeau, J. Power Sources 2007, 174, 462.
- [30] R. Tao, T. Zhang, S. Tan, C. J. Jafta, C. Li, J. Liang, X. Sun, T. Wang, J. Fan, Z. Lu, C. A. Bridges, X. Suo, C. Do-Thanh, S. Dai, Adv. Energy Mater. 2022, 12, 2200519.
- [31] H. Lyu, J. Li, T. Wang, B. P. Thapaliya, S. Men, C. J. Jafta, R. Tao, X.-G. Sun, S. Dai, ACS Appl. Energ. Mater. 2020, 3, 5657.
- [32] T. Hu, J. Tian, F. Dai, X. Wang, R. Wen, S. Xu, J. Am. Chem. Soc. 2023, 145, 1327.
- [33] S. Chen, R. Tao, J. Tu, P. Guo, G. Yang, W. Wang, J. Liang, S. Lu, Adv. Funct. Mater. 2021, 31, 2101199.
- [34] R. Tao, G. Yang, E. C. Self, J. Liang, J. R. Dunlap, S. Men, C. Do-Thanh, J. Liu, Y. Zhang, S. Zhao, H. Lyu, A. P. Sokolov, J. Nanda, X. Sun, S. Dai, Small 2020, 16, 2001884.
- [35] L. Madec, R. Petibon, K. Tasaki, J. Xia, J.-P. Sun, I. G. Hill, J. R. Dahn, Phys. Chem. Chem. Phys. 2015, 17, 27062.
- [36] C. Guo, Y. Guo, R. Tao, X. Liao, K. Du, H. Zou, W. Zhang, J. Liang, D. Wang, X. G. Sun, S. Y. Lu, Nano Energy 2022, 96, 107121.
- [37] K. Du, R. Tao, C. Guo, H. Li, X. Liu, P. Guo, D. Wang, J. Liang, J. Li, S. Dai, X. G. Sun, Nano Energy 2022, 103, 107862.
- [38] J. Arai, A. Matsuo, T. Fujisaki, K. Ozawa, J. Power Sources 2009, 193, 851.
- [39] J. Kim, H. Kim, J. H. Ryu, S. M. Oh, J. Electrochem. Soc. 2020, 167, 080529.
- [40] L. Li, S. Zhou, H. Han, H. Li, J. Nie, M. Armand, Z. Zhou, X. Huang, J. Electrochem. Soc. 2011, 158, A74.
- [41] J. P. Christophersen, DOE Rep. 2015. https://inldigitallibrary.inl.gov/sites/ sti/sti/6492291.pdf.

Manuscript received: July 5, 2023 Revised manuscript received: August 4, 2023 Version of record online: August 23, 2023